Submillimeter Array Technical Memorandum

Number: 17
Date: 19 June 1990
From: B. Bruckman and B. Davis

Aluminum Panel Study

Summary

We have studied the dimensional stability of machined aluminum panels when exposed to machining, gravity, thermal, and wind environments. We used a modification of the outer panel (largest panel) of the Hatcreek 20 foot antenna for our baseline design. Results are summarized in Table 1. The effect of errors for the gravity load case could be reduced further by evaluating them relative to a best-fit parabola. The errors for the machining load could be reduced to less than 7 microns RMS by using an iterative machining and measuring process to reduce the effects of spring back and/or by adding additional stiffening ribs.

We found that behavior for the thermal load cases depends strongly on the surface treatment of the panels, the site environment, and any coefficient of thermal expansion (CTE) mismatch between the backup structure and the panels. With no subreflector movement for corrections, the approximate effective reflector tolerance (ERT) for the seasonal/diurnal temperature effects is on the order of 3600 microns RMS (assuming an all aluminum structure). An active secondary and temperature sensors will be required to correct this effect, if we use aluminum panels. The approximate ERT due to CTE mismatch between the backstructure and the panels for diurnal/seasonal effects is on the order of 3 to 5 microns RMS assuming a steel backstructure. The approximate ERT for thermal gradients through the panel is on the order of 3 to 12 microns RMS assuming a 1-3 degree F gradient. This error can be reduced by changing the rib design and/or insulating the back of the panel. (Note: Adding insulation to the backs of the panels will probably cause gradients across the entire dish to increase.)

In addition to the errors introduced by the behavior of a single panel, there will be pointing as well as surface errors due to thermal gradients across the entire reflector. These effects will be studied later when a model of the entire reflector with backstructure is assembled. After these studies we will be able to fully assess the viability of machined aluminum panels for the SMA antennas.

Case	Approximate Effective Reflector Tolerance (ERT) (microns, RMS)
Wind load	1.2
Gravity	2.0
Machining	14 *
Seasonal/diurnal thermal	3-5
Thermal gradient	3-12

Table 1: Summary of results

* The ERT for the machining load can be reduced to less than 7 microns RMS by using an iterative machining and measuring process to reduce the effects of spring back or by adding additional stiffening ribs.

Introduction

Historically, aluminum has been the material selected for constructing reflector panels for radio telescopes. Its corrosion resistance, workability, conductivity, and structural properties make it an ideal choice in many ways. The one drawback which aluminum has is its relatively high coefficient of thermal expansion (approximately two times that of steel and 3 to 12 times that of carbon fiber composites). This may limit the accuracy of aluminum panels because variations in temperature and temperature gradients may cause relatively large thermal distortions.

Most high accuracy aluminum panel designs have used bonded construction to allow production of many panels from a single high accuracy mold. This construction technique magnifies thermal distortion because temperature gradients across the depth of the panel are increased in magnitude due to the relatively high thermal resistance of the bond line (aluminum conductivity = .53 cal/cm-sec-°C vs. Hysol 9430 epoxy conductivity = .000425 cal/cm-sec-°C). To reduce this effect, the Hatcreek antennas use a machined aluminum panel so that there is no bond line. With the high thermal conductivity of aluminum, this design may yield a basically isothermal panel. The purpose of this study is create a structural model of the Hatcreek panel design to determine if this approach can be used for the SMA antennas.

Finite Element Model (FEM) Description

The Hatcreek outer panel is shown in Figure 1. The panel geometry was approximated as a section of a hemispherical shell with a radius of 5.57 meters (this deviates from the parabolic shape by less than one inch and has negligible effect on the structural behavior of the model). The inner edge of the panel is defined at a radius of 93 inches from the central axis and the outer edge is defined at a radius of 120 inches. The included angle of the panel is 15 degrees for the Hatcreek antennas. The initial model used this included angle. To reduce gravity, wind, and machining load deflections the included angle was reduced to 10 degrees and the inner and outer radii were changed to 98 and 120 inches respectively. The final model is shown in Figure 2. (Note: It would probably be possible to reduce these deflections by optimizing the location and size of the stiffening ribs without reducing the included angle of the panel. This may be a better approach for a final design.)

The panel was modeled using the ANSYS finite element program. Only half of the panel was modelled because a plane of symmetry exists for the structure and all load cases we examined. The panel surface and stiffening ribs were modeled with STIFF 63 type elements for the wind, gravity, and machining load cases. STIFF 43 elements were used for the thermal load cases because we found that the latest version of ANSYS gives unreliable results for STIFF 63 type elements for thermal load cases. The thickness used for the panel elements was 0.125 inches and the stiffener elements used a thickness of 0.125 inches to approximate the average thickness of the stiffening ribs. The model is restrained at the plane of symmetry to include the effects of the other half of the structure and at two corners on the back of the stiffening ribs to represent the mounting of the panel to the back structure. The Hatcreek panels are actually supported at points which do not coincide with the stiffening ribs. We found that performance is improved significantly when the panel support points coincide with the stiffening ribs and have used this approach in the model. Kinematic restraints are applied at the support points so that thermal load cases produce a stress free condition.

The ERT is approximated using the methods of Ruze [1] by taking the peak normal-to-surface error, multiplying by a correction factor for the reflector curvature, and taking one third of the result. The correction factor used is .85 which corresponds to an f/D of .42 for the Hatcreek reflector.

Wind Load Case

A .00893 psi static pressure was applied normal to the front surface of the panel to simulate a 10 m/s (22.4 mph) wind at an altitude of 10,000 feet and a temperature of 20° F (drag coefficient assumed as 1.3). For this loading the peak, normal-to-surface (PNS) deflection was 4.2 microns and the approximate effective reflector tolerance was 1.2 microns RMS. A contour map of the model deflections is shown in Figure 3. The performance for this load case and the gravity and machining load cases could be improved significantly by optimizing the size and the

position of the stiffening ribs.

Gravity Load Case

A 1g static load was applied normal to the plane formed by the four panel support points. This is a worst case condition for gravity deflections. This gives a maximum PNS deflection of 7.1 microns and an approximate effective reflector tolerance of 2.0 microns RMS. A contour map of the deflections is shown in Figure 4. In actual practice this error can be reduced significantly if the final machining is done with the panel supported at its support points and the gravity vector oriented perpendicular to the plane of the support points. Then the gravity deflections for this position relative to the theoretical surface are zero and the errors for other attitudes of the gravity vector will be relatively less.

Machining Load Case

Two load cases were run: a 5 lb load applied at the center of the panel normal to the surface (this point lies along a rib) and a 5 pound load at the center of an area framed by the stiffening ribs. The second case gave worst case deflections with the maximum PNS deflection being 51 microns and the approximate effective reflector tolerance being 14 microns RMS. A contour map of the deflections for this case is shown in Figure 5. These results assume that no special provisions were taken to eliminate the effects of spring back. If we use this approach, we will have to stiffen the panel sufficiently or perform an iterative machining/measuring process or do both.

Thermal Load Cases

Two thermal load cases were considered: a temperature gradient through the depth of the panel and an overall change in the ambient temperature of the entire antenna structure i.e. a diurnal/seasonal effect. A temperature gradient through the depth of the panel occurs anytime heat flows into, out of, or through the panel. If the panel was of uniform thickness and did not have stiffening ribs, the temperature gradient would be negligible because of the high thermal conductivity of the aluminum. However, the stiffening ribs behave in a way which is analogous to a fin on a heat sink. This causes a significant temperature difference between the tip of the stiffening rib and the surface of the panel.

The error introduced by this effect is related to the size of the panel and the magnitude of the gradient. Figure 6 shows approximate PNS error vs. maximum panel dimension (across a diagonal) for various magnitudes of temperature gradient. The PNS error was approximated by calculating the maximum out of plane displacement for a flat rectangular plate with the various temperature gradients applied through the thickness of the plate. Figure 7 shows the deflected shape for the FEM with a 1 degree F linear gradient (.28 deg F / inch) applied through the stiffening ribs. The effective reflector tolerance for this case is approximately 3.4 microns RMS

and the maximum PNS deflection is 12 microns. The exact temperature gradient which will be induced during operation is difficult to predict, but it will be on the order of 1 to 3 degrees F. If we use aluminum panels this effect will probably limit our maximum panel size or we may have to use active or passive thermal controls on the panels.

For an overall change in the ambient temperature of the structure (i.e. a diurnal/seasonal effect), the error depends on the difference in CTE of materials used for the back structure, the panels, and the subreflector support. Assuming an aluminum back structure, aluminum panels, and carbon fiber subreflector support with a CTE of approximately zero results in a pure focus error which can be corrected by measuring the temperature of the structure and moving the subreflector to account for temperature changes. Without correction the effective reflector tolerance for this case is 1020 microns RMS for a temperature change of 50 degrees F and it is clear that we must perform the correction. 50 degrees F is a reasonable assumption for seasonal temperature fluctuations of the structure given fluctuations of ambient air temperatures of +/- 20 to +/-30 deg F and temperature deltas between the structure and the ambient air on the order of 20 to 30 degrees F due to solar heating or nighttime radiation cooling.

Figure 8 shows the predicted temperature rise above ambient air temperature as a function of solar heat absorbed by a panel of uniform thickness or sufficiently away from a stiffening rib which would act as a fin. The upper curve is for a bare aluminum panel, with an emissivity of 0.1 for the front and back surface. The lower curve is for an aluminum panel with its back surface coated with high emissivity paint (emissivity of .8). The heat absorbed by the panel is plotted on the x-axis. It depends on the absorptance of the panel and the solar heat load (assumed as 300 Btu/hr/ft^2) . Points one and two are for sun shining on an unpainted aluminum surface with an assumed absorptance of .15 giving a heat load of 45 Btu/hr/ft^2/deg F and temperature rises of 20 deg F for the painted case and 28 deg F for the unpainted case. Point three is for sun shining on the painted back surface with an absorptance of .35 giving a heat load of 105 Btu/hr/ft^2/deg F and a temperature rise of 43 deg F. Similar temperature deltas will also occur at night.

When the back structure CTE and the panel CTE are not the same, additional surface errors for temperature changes in the antenna structure occur. If we assume that the panels are attached to the back structure in a manner that allows the panels to expand and contract without introducing loads into the panels, the reflector support points will move in accordance with the coefficient of thermal expansion (CTE) of the backstructure while the reflector panels will grow (or shrink) in accordance with their CTE. The result is that the individual panel surfaces have deformed to a new parabola in accordance with the panel CTE, but they are positioned in accordance with the back structure CTE. If it is assumed that we move the subreflector to account for the change in the back structure, then the error from this effect is the deviation of the individual panel surfaces from the parabola to which the reflector support points have moved.

The magnitude of this error is a function of the temperature change, the size of the panels, and the difference in CTE's for the panels and the back structure. Figure 9 illustrates the peak surface error for an aluminum panel (CTE = 12.8E-6 in/in/°F) mounted to a steel back structure (CTE = 6.5E-6 in/in/°F) as a function of panel size and temperature change. It should be noted that

these curves assume that both the panels and the backstructure are at the same temperature and that the temperature change is relative to the ambient temperature when the panels were set.

Conclusions

The preliminary ERT budget for the SMA antenna is shown in Table 2. If an iterative machining process is assumed and the worst case ERT's for thermal effects from Table 1 are combined as a root-sum-squared (RSS) to give the thermal contributor for panels, the ERT budget would be as shown in Table 3. If the best case numbers for thermal effects from Table 1 are used the ERT budget would be as shown in Table 4. The goal for the SMA antenna is an ERT of 15 microns RMS. It appears that we can use aluminum panels and meet the 15 micron RMS goal, but the maximum panel size will have to be limited and the thermal gradients will have to be controlled. Also, the effects of thermal gradients across the entire dish have not been considered. These effects may degrade performance or limit our design options to the point where aluminum panels are not a viable option.

	ERT source	ERT in microns (inches) RMS	
Panels:			
	Manufacturing	7	0.00028
	Alignment	7	0.00028
	Wind	3	0.00012
	Gravity	3	0.00012
	Thermal	3	0.00012
Backstructure:			
	Wind	4	0.00016
	Gravity	6	0.00024
	Thermal	6	0.00024
	RSS total	14.59	

Table 2. Preliminary ERT budget.

	ERT source	ERT in microns (inches) RMS	
Panels:			
	Manufacturing	7	0.00028
	Alignment	7	0.00028
	Wind	1.2	0.000048
	Gravity	2	0.00008
	Thermal	13	0.00052
Backstructure:			
	Wind	4	0.00016
	Gravity	6	0.00024
	Thermal	6	0.00024
	RSS total	18.99	

Table 3. ERT budget using worst case ERT for thermal effects from Table 1.

	ERT source	ERT in microns (inches) RMS	
Panels			
	Manufacturing	7	0.00028
	Alignment	7	0.00028
	Wind	1.2	0.000048
	Gravity	2	0.00008
	Thermal	4.2	0.000168
Backstructure			
	Wind	4	0.00016
	Gravity	6	0.00024
	Thermal	6	0.00024
	RSS total	14.46	

Table 4. ERT budget using best case ERT for thermal effects from Table 1.

References

[1] J. Ruze, "Antenna tolerance theory," Proc. IEEE, vol. 54, pp.633-640, Apr. 1966

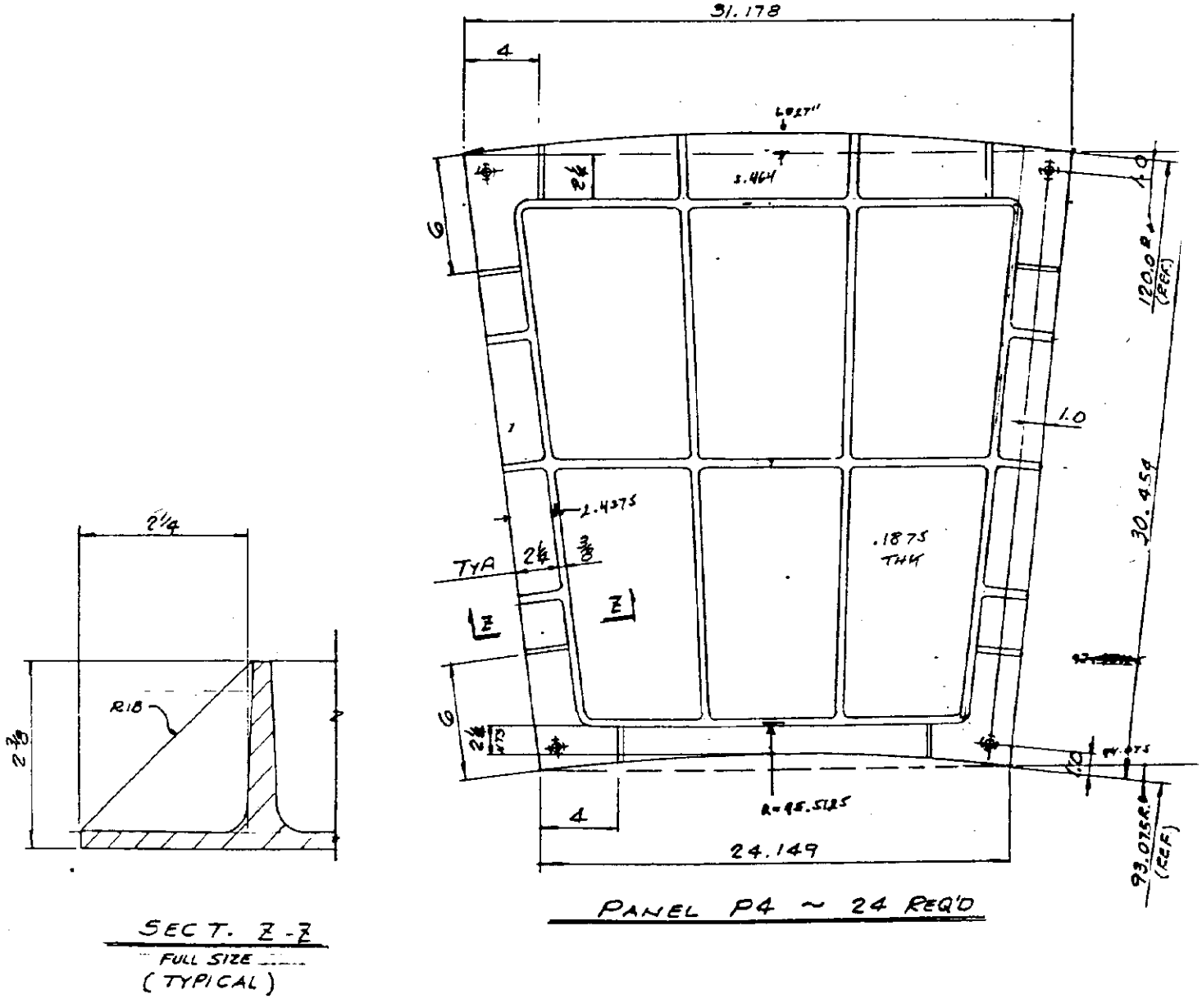

Figure 1. Hatcreek outer panel design.

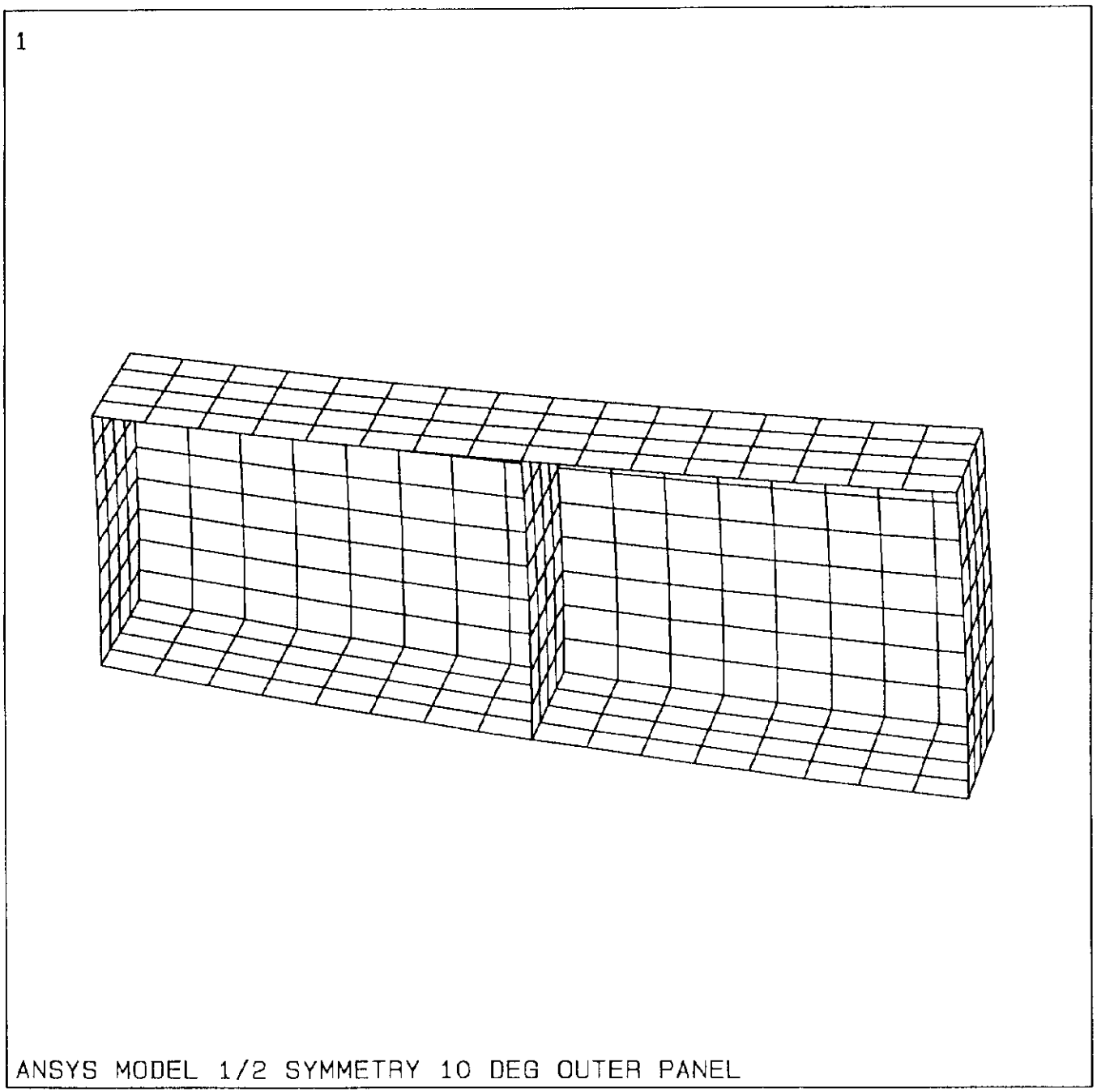

Figure 2. Finite element model.

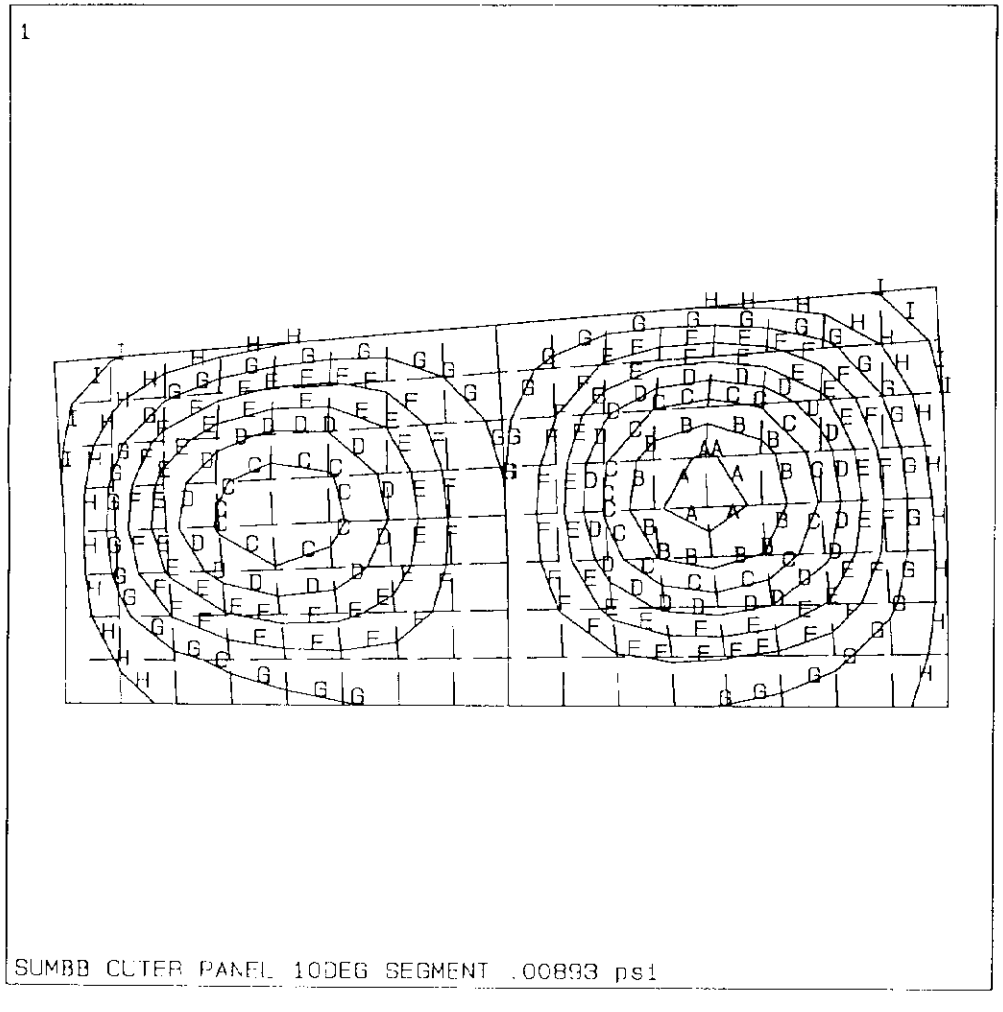

Note: Deflections are in inches.

Figure 3. Contour plot of normal-to-surface deflections for .00893 psi static pressure load to simulate a 10 m/s (22.4 mph) wind at an altitude of 10,000 feet and a temperature of 20° F (drag coefficient assumed as 1.3).

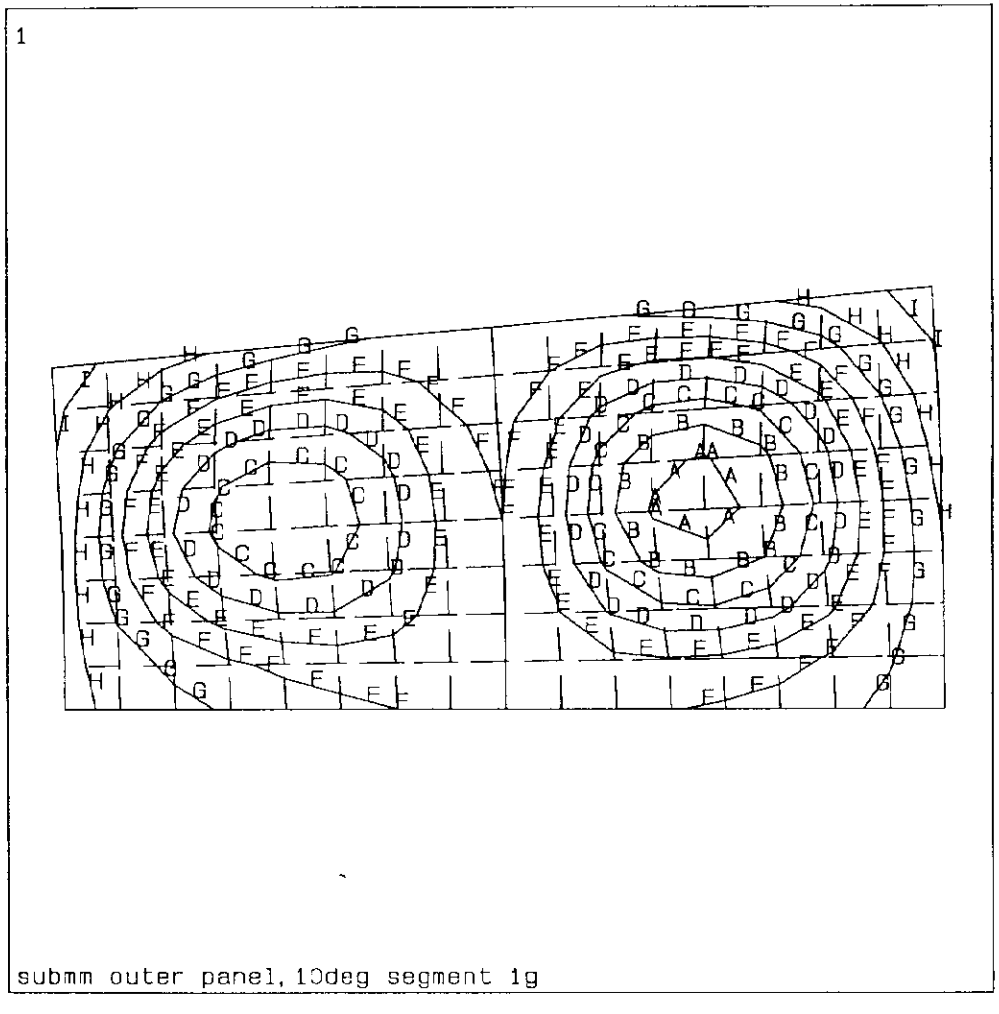

ANSYS 4.4
MAY 7 1990
13: 05: 13
PLOT NO. 1
POST1 STRESS
STEP=1
ITER=1
UX
CSYS=2
DMX =0.283E-03
SMN =-0.282E-03
SMX =0.185E-13

ZV =1
DIST=12.306
XF =108.813
YF =5.229
ZF =190.102
A =-0.267E-03
B =-0.235E-03
C =-0.204E-03
D =-0.173E-03
E =-0.141E-03
F =-0.110E-03
G =-0.784E-04
H =-0.471E-04
I =-0.157E-04

Note: Deflections are in inches.

Figure 4. Contour plot of normal-to-surface deflections for gravity load.

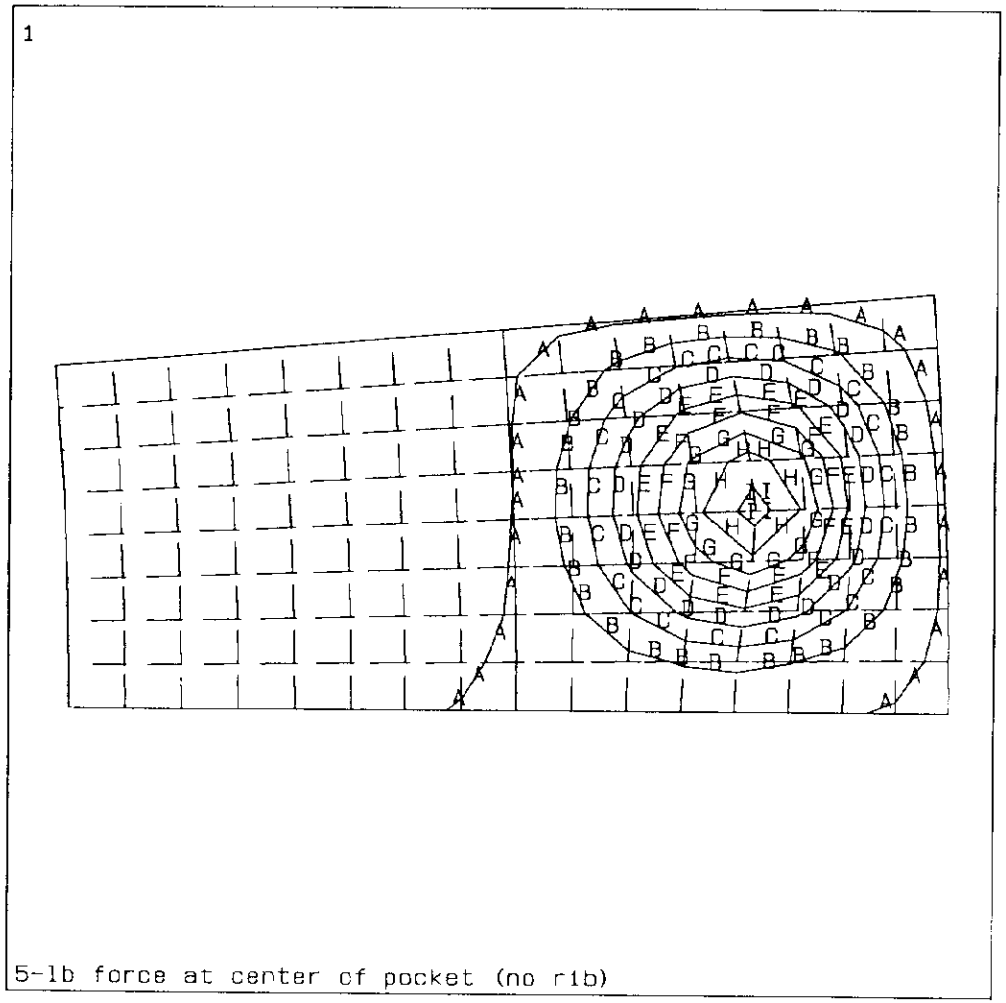

Note: Deflections are in inches.

Figure 5. Contour plot of normal-to-surface deflections for 5 lb machining load at the center of an area framed by the stiffening ribs.

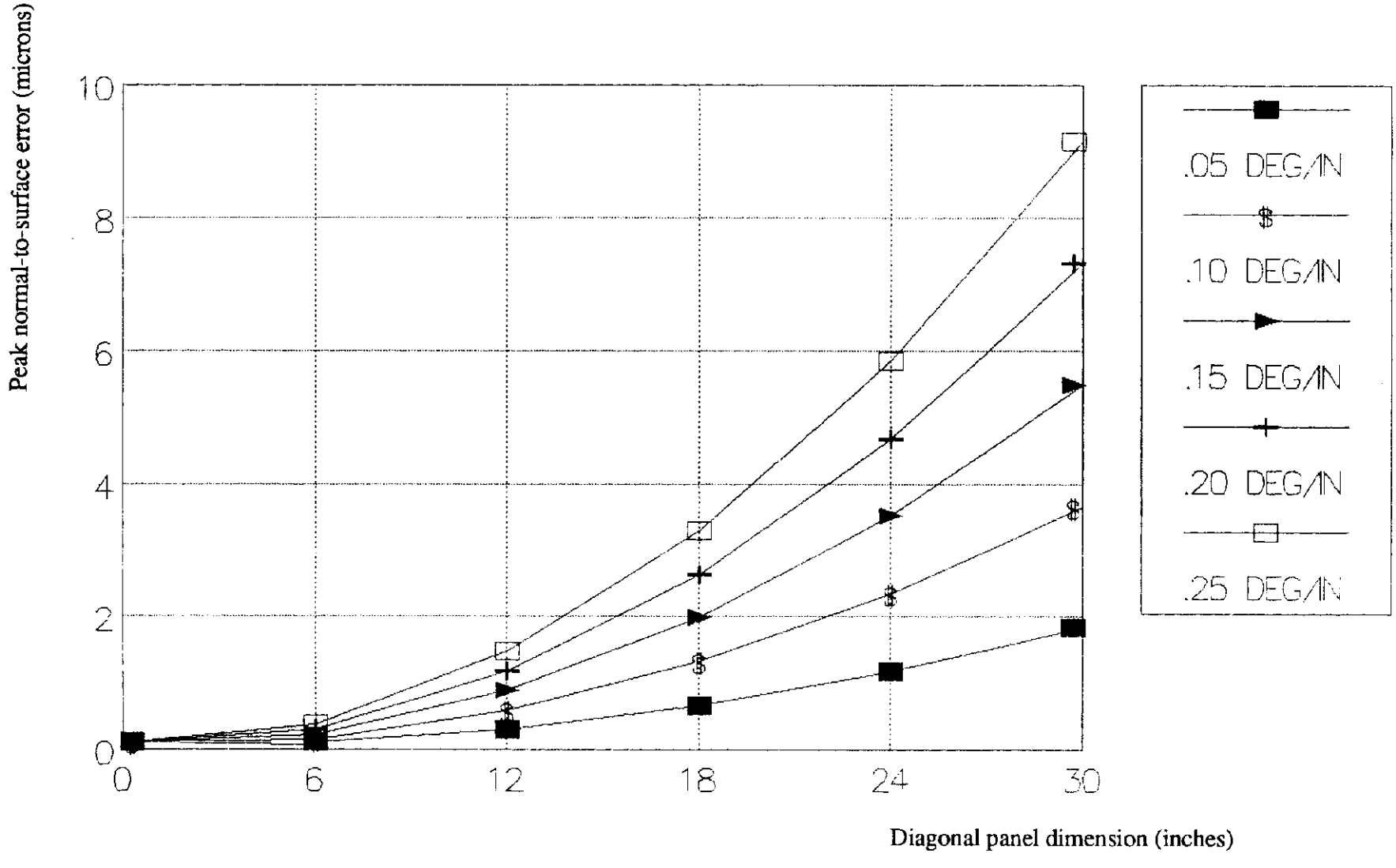

Figure 6. Approximate PNS error vs. maximum panel dimension (across a diagonal) for various magnitudes of temperature gradient.

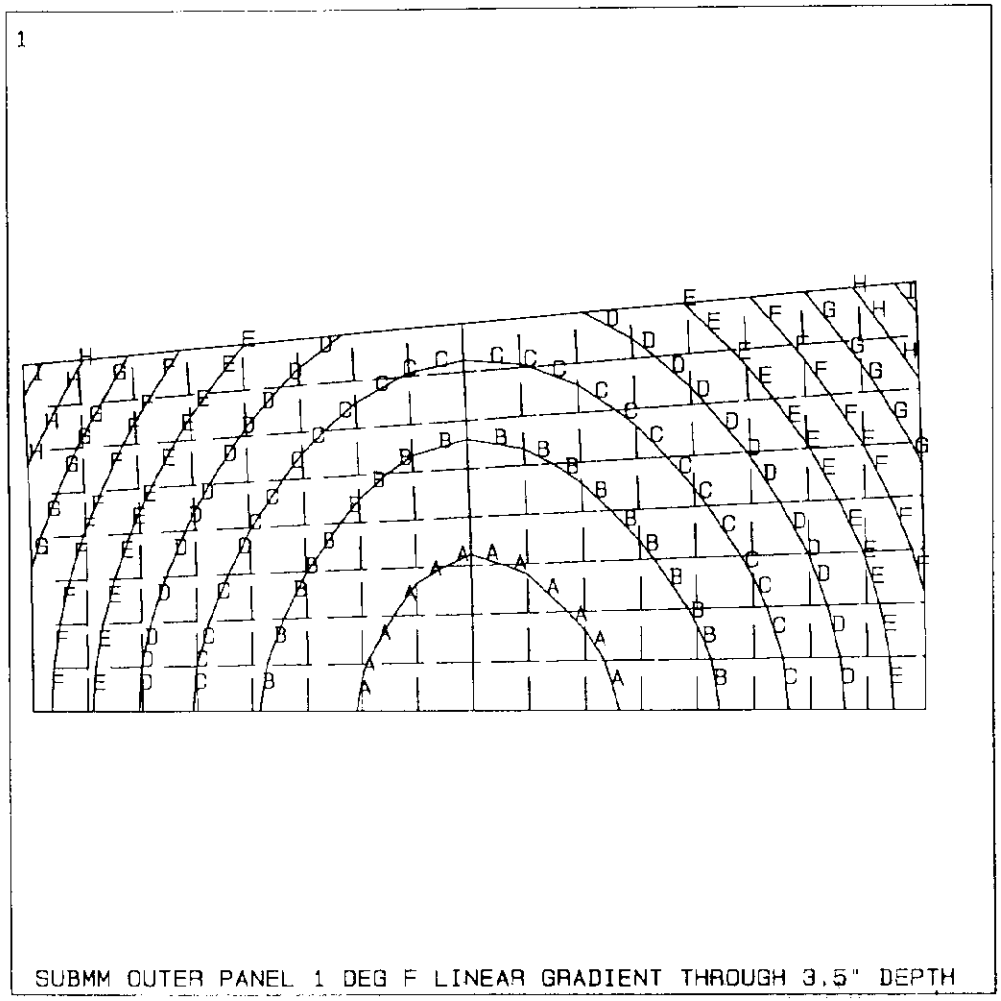

ANSYS 4.4
MAY 3 1990
11:53:52
PLOT NO. 1
POST1 STRESS
STEP=1
ITER=1
UX
CSYS=2
DMX =0.544E-03
SMN =-0.473E-03
SMX =0.344E-11

ZV =1
DIST=12.306
XF =108.813
YF =5.229
ZF =190.102
A =-0.447E-03
B =-0.395E-03
C =-0.342E-03
D =-0.289E-03
E =-0.237E-03
F =-0.184E-03
G =-0.132E-03
H =-0.789E-04
I =-0.263E-04

Note: Deflections are in inches.

Figure 7. Contour plot of normal-to-surface deflections for a 1 degree F gradient (.28 deg F / inch) applied through the stiffening ribs.

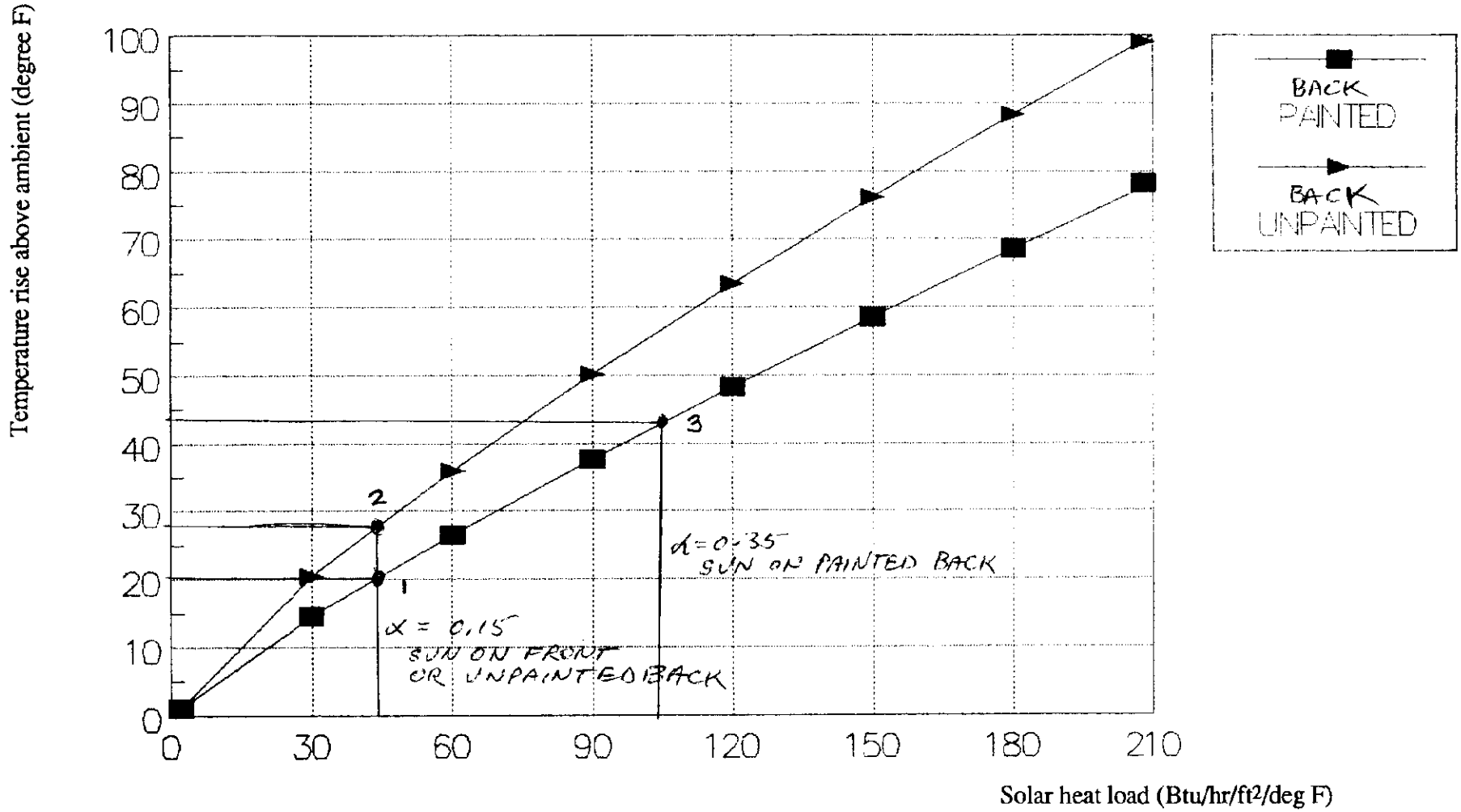

Figure 8. The predicted temperature rise above ambient air temperature as a function of solar heat absorbed by a panel of uniform thickness or sufficiently away from a stiffening rib which would act as a fin.

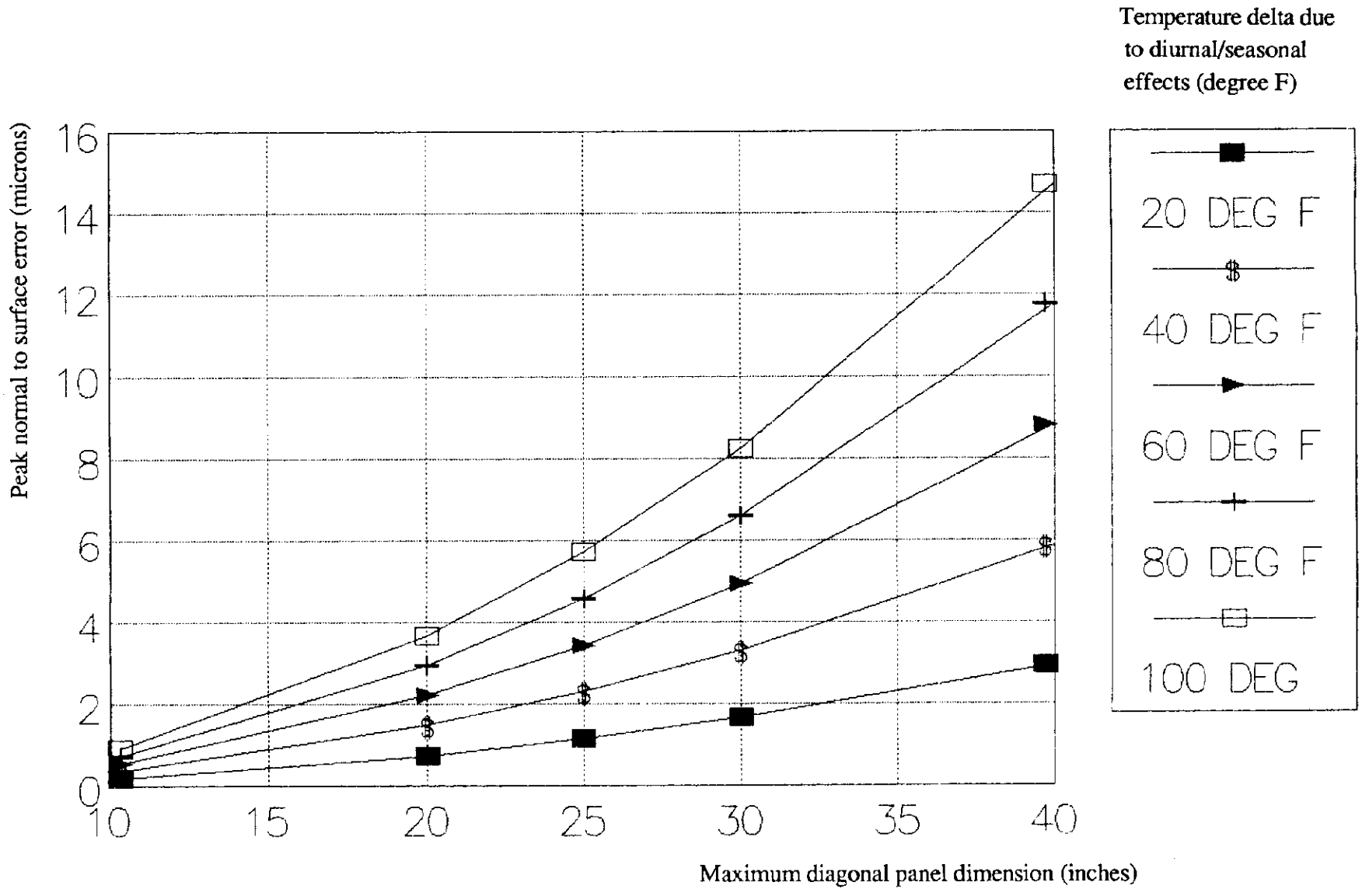

Figure 9. The PNS error for an aluminum panel (CTE = 12.8E-6 in/in/°F) mounted to a steel back structure (CTE = 6.5E-6 in/in/°F) as a function of panel size and temperature change.